

# **Quantification and rationalization of the higher affinity of sodium over potassium to protein surface**

**Luboš Vrbka, Jiří Vondrášek, Barbara Jagoda-Cwiklik, Robert Vácha, and Pavel Jungwirth\***

*Institute of Organic Chemistry and Biochemistry, Academy of Sciences of the Czech Republic, and Center for Biomolecules and Complex Molecular Systems, Flemingovo nám. 2, 16610 Prague 6, Czech Republic*

*\*Corresponding author: Pavel.Jungwirth@uochb.cas.cz*

**Classification:** Biological Sciences – Biophysics/Biochemistry

**Manuscript Information:** 21 (double spaced) pages, 2 figures, and 2 tables. Total number of characters: 29,404.

## Abstract

For a series of different proteins, including a structural protein, enzyme, inhibitor, protein marker, and a charge transfer system, we have quantified the higher affinity of  $\text{Na}^+$  over  $\text{K}^+$  to the protein surface by means of molecular dynamics simulations and conductivity measurements. Both approaches show that sodium binds at least twice as strongly to the protein surface as potassium, this effect being present in all proteins under study. Different parts of the protein exterior are responsible to a varying degree for the higher surface affinity of sodium, with the charged carboxylic groups of aspartate and glutamate playing the most important role. Local ion pairing is, therefore, the key to the surface preference of sodium over potassium, which is further demonstrated and quantified by simulations of glutamate and aspartate in the form of isolated amino acids, as well as short oligopeptides. As a matter of fact, the effect is already present at the level of preferential pairing of the smallest carboxylate anions, formate or acetate, with  $\text{Na}^+$  vs  $\text{K}^+$ , as shown by molecular dynamics and ab initio quantum chemical calculations. By quantifying and rationalizing the higher preference of sodium over potassium to protein surface the present study opens a way to molecular understanding of many ion-specific (Hofmeister) phenomena involving protein interactions in salt solutions.

## Introduction

Sodium and potassium represent the two most abundant monovalent cations in living organisms. Despite the fact that they possess the same charge and differ only in size ( $\text{Na}^+$  having a smaller ionic radius but larger hydrated radius than  $\text{K}^+$  (1)), sodium vs potassium ion specificity plays a crucial role in many biochemical processes. More than hundred years ago, Hofmeister discovered that  $\text{Na}^+$  destabilizes (salts out) hens' egg white protein more efficiently than  $\text{K}^+$  (2), analogous behavior being later shown also for other proteins (3). In a similar way, sodium was found to be significantly more efficient than potassium, e.g., in enhancing polymerization of rat brain tubulin (4).  $^{23}\text{Na}$  NMR studies were also used to characterize cation-binding sites in proteins (5). The vital biological relevance of the difference between  $\text{Na}^+$  and  $\text{K}^+$  is exemplified by the low intracellular and high extracellular sodium/potassium ratio maintained in living cells by ion pumps at a considerable energy cost (6). The principal goal of this paper is to quantify and rationalize the different affinities of sodium and potassium to protein surfaces by means of molecular dynamics simulations, quantum chemistry calculations, and conductivity measurements for a series of proteins and protein fragments in aqueous solutions. Our effort, which is aimed at understanding the generic, thermodynamic  $\text{Na}^+/\text{K}^+$  ion specificity at protein surface, is thus complementary to recent computational studies of ion selectivity during active transport across the cellular membrane (7-10).

Since primitive continuum electrostatic models, which are still widely used to describe solvation of biomolecules, cannot distinguish between sodium and potassium, their ion specificity at protein surfaces has been to a large extent ignored (11). Unlike divalent cations

such as  $\text{Ca}^{2+}$  with well recognized specific binding to proteins (6),  $\text{Na}^+$  and  $\text{K}^+$  ions are often viewed as merely defining the ionic strength of the corresponding salt solution (11). This is also due to the fact that the specificity of ions in solutions is traditionally discussed in terms of their kosmotropic (water structure making) vs chaotropic (water structure breaking) behavior (12). In this respect sodium and potassium, which are next to each other in the Hofmeister series, are roughly neutral, the former being a very weak kosmotrope and the latter a weak chaotrope (11). Moreover, recent spectroscopic measurements in electrolyte solutions showed that the effect of dissolved monovalent ions does not propagate beyond the first solvation shell (13), which underlines the importance of local ion-ion, ion-water, and water-water interactions over long range solvent ordering effects. In this spirit, the so called Law of matching water affinities (11, 14, 15) has been recently proposed as an attempt to explain, among others, the  $\text{Na}^+/\text{K}^+$  ion specificity. In a nutshell, based on simple electrostatic arguments it has been suggested that a cation and an anion with similar (either large or small) hydration energies tend to form contact ion pairs in aqueous solutions. Within this qualitative concept, sodium matches better than potassium in surface charge density (and in the related hydration energy) major intracellular anions or anionic groups, such as carboxylate, carbonate, and the phosphate monoanion (15). It has been argued that  $\text{Na}^+$  would thus binds more strongly than  $\text{K}^+$  to protein surfaces containing  $\text{COO}^-$  groups, which may be one of the reasons why sodium has to be pumped out of the cell (11).

## **Results**

In the present study, we systematically investigated the ion specific behavior of sodium and potassium at protein surfaces. To this end we performed extensive molecular dynamics

(MD) simulations of a series of five very different proteins in aqueous mixtures of NaCl and KCl (containing typically 0.25 M of each salt). We chose two extracellular and three intracellular proteins. As the former we took actin as a representative of structural proteins and bovine pancreatic trypsin inhibitor (BPTI) as an enzyme inhibiting protein. Among the latter, ubiquitin was taken as a typical protein marker, hyperthermophilic rubredoxin as an electron transfer system, and ribonuclease (RNase) A as a model enzyme. Our computational findings were supported by conductivity measurements of aqueous solutions of NaCl and KCl with added protein. The measured proteins were RNase A and bovine serum albumin (BSA). The Na<sup>+</sup> vs K<sup>+</sup> ion specific behavior was further rationalized by means of additional simulations of solvated oligopeptides and individual amino acids containing at pH = 7 a carboxylate group in the side chain (i.e., aspartate (Asp) and glutamate (Glu)), as well as by MD and ab initio calculations of ion pairing of alkali cations with small carboxylate anions (formate and acetate). All the studied systems together with the computational and experimental methods are described in detail in the Materials and Methods section.

Figure 1 summarizes the principle results of MD simulations for the five proteins under study. It shows the distributions of sodium and potassium cations in the vicinity of the protein and the integrals thereof, i.e., cumulative sums providing the number of Na<sup>+</sup> and K<sup>+</sup> ions within a certain distance from the protein surface. Both distributions exhibit a peak (Na<sup>+</sup> at 2.3 and K<sup>+</sup> at 2.8 Å from the protein surface) and, correspondingly, there is a plateau region for the cumulative sums, which defines the number of ions in the immediate vicinity of the protein. The crucial result is that in all cases there are about twice as many (or even more) sodium than potassium cations near the protein surface. In absolute numbers, there are on average 1- 4 Na<sup>+</sup> ions at the protein surface, except for BPTI where this number is several times smaller (Figure 1).

From the left three columns in Figure 1 we see that the preference of  $\text{Na}^+$  over  $\text{K}^+$  for the protein surface comes mainly from cation-specific interactions with the side chain carboxylate groups, with contributions also from the backbone and, to a lesser extent, from other side chain groups. The ion specificity at the backbone is primarily due to interactions with the carbonyl oxygen of the amide group, while the selectivity at other side chain groups can also have some contribution from cation-aromatic ring interactions in phenylalanine. The latter interactions were recently shown to be stronger for  $\text{Na}^+$  than  $\text{K}^+$  as well (16), however, they cannot be described accurately within standard force fields. The very different nature and amino acid content of the proteins under study is reflected in varying total numbers of ions at the protein surface and relative contributions from different protein parts, however, the higher surface affinity of  $\text{Na}^+$  over  $\text{K}^+$  is revealed as a generic property for all investigated proteins.

The above computational results are supported by conductivity measurements in NaCl and KCl solutions of varying concentrations with added RNase A (as one of the simulated proteins) or BSA (which is easily available but too large and without well determined structure to be effectively simulated). For both proteins, the relative decrease in conductivity is significantly larger in NaCl compared to KCl solutions (Figure 2), which can be directly interpreted in terms of sodium being more efficiently removed from the solution to the protein surface than potassium ions. Assuming that the decrease in conductivity is solely due to ions adsorbed at the protein surface, we can deduce that, e.g., for RNase A one protein molecule effectively binds about 1 – 2 sodium cations, while it attracts less than half the amount of potassium ions. These numbers, which are only weakly dependent on salt concentration, agree well with the above results from MD simulations in solutions with a higher ionic strength. The

results of conductivity measurements for BSA (the small undulation on the KCl curve being within the statistical error - Figure 2b) can be interpreted in a quantitatively similar way.

Specific ion effects at protein surfaces, particularly for higher salt concentrations, are often rationalized in terms of surface tension changes invoked by the presence of a given salt (14, 17, 18). The analogy between air-water and protein-water interfaces can be good for the exposed hydrophobic patches of the protein with low polarity and dielectric constant, however, it is much less operative for the polar or charged hydrophilic parts of protein surface. Moreover, unlike for anions, ion-specific effects for cations at the air-water interface are negligible with sodium and potassium salts having almost the same surface tension vs concentration curves (19). This is consistent with the present picture indicating that the ion specificity originates to a large extent from local interactions with charged and polar groups at the protein surface (20). In particular, the higher affinity of sodium over potassium for the protein surface comes mainly from specific interactions with the carboxylate groups within the amino acid side chains.

In order to further verify and quantify the above conclusion, we have focused on the sodium and potassium affinity to the relevant protein fragments by simulating the two amino acids containing at pH = 7 the COO<sup>-</sup> group in the side chain. Glu and Asp were studied in a mixed NaCl and KCl solution as isolated amino acids, as well as short oligopeptides, all capped using the acetyl and methylamide groups at the N- and C-termini, respectively. The principal results of these simulations are summarized in Table 1. Consistently with the results for proteins (Figure 1), the Na<sup>+</sup>/K<sup>+</sup> ratios reveal a 2-4 times stronger preference of sodium over potassium for the oligopeptide or amino acid surface (Table 1). This relative preference of Na<sup>+</sup> is found both at the side chains and near the backbone. The former play a more important role in absolute

terms since they represent ion-ion interactions, while the latter only weaker ion-dipole interactions involving the polar C=O group of the amide.

We further reduced the problem of the alkali cation - side chain carboxylate interaction to a question concerning the relative strength of pairing of Na<sup>+</sup> and K<sup>+</sup> with acetate anion. To this end, we simulated an aqueous mixture of acetate, sodium, potassium, and chloride, following the acetate-alkali ion pairing patterns. There is a clear preference of Na<sup>+</sup> over K<sup>+</sup> for the vicinity of acetate, reaching a value of 3.4 in relative terms (Table 1). For the two smallest carboxylate anions, formate and acetate, we were also able to perform ab initio quantum chemical calculations of pairing with sodium or potassium, employing a polarizable continuum model for water (see Materials and Methods for further computational details). Within these calculations, pairing with Na<sup>+</sup> is favored over that with K<sup>+</sup> by more than 2 kcal/mol, both for formate and acetate (Table 2). The ab initio results thus support the conclusions from classical MD simulations, indicating an even stronger relative affinity of Na<sup>+</sup> over K<sup>+</sup> to the COO<sup>-</sup> group. They are also in accord with larger decrease in water activity in aqueous sodium acetate compared to potassium acetate, although this effect is relatively small at low concentrations. In a similar spirit, analogous ab initio calculations of pairing of alkali cations with formaldehyde reveal a free energy preference of about 1 kcal/mol in favor of sodium over potassium. This supports the MD results concerning ion selectivity at the protein backbone region due to specific interactions with the carbonyl oxygen of the amide group.

## Discussion and Conclusions

Present results provide a clear and quantitative picture of the preference of sodium over potassium for protein surfaces, rationalizing this effect primarily in terms of local cation-specific interactions with the anionic carboxylate group in Glu and Asp side chains. Additional contributions to the  $\text{Na}^+/\text{K}^+$  selectivity come from interactions with carbonyl oxygens of the amide constituting the protein backbone and, to a much smaller extent, from other side chain groups. We do not observe a qualitative dependence of the effect on salt concentration, which can be related to the local character of the  $\text{Na}^+$  vs  $\text{K}^+$  selectivity. This is different from specific effects of anions at protein surfaces, which may exhibit even a reversal of Hofmeister ordering upon increasing salt concentration (17, 21). The importance of alkali cation–protein interactions for “in vitro” experiments can be often hidden behind experimental conditions optimized for a particular practical task. Nevertheless, “in vivo” conditions directly point to the importance of these effects, which can play a very special or even crucial role in processes where protein–protein intermolecular as well as intramolecular interactions are important, such as protein folding or build up of protein functional networks. There is ample experimental evidence concerning alkali salt effects on protein folding (22, 23). It is also well known that the mostly hydrophilic surfaces of non-membrane proteins are involved in protein-protein interaction within various intra- and extra-cellular processes (24, 25). The number of charged groups on the protein surface which mediate these interactions is high, and these sites are also accessible to interactions with small monovalent ions, such as  $\text{Na}^+$  and  $\text{K}^+$ . Increasing the concentration of an ion with a higher affinity to the protein effectively modulates its interaction strength and even functionality (20, 26). The present simulation and experimental results, quantifying the stronger binding of  $\text{Na}^+$  to protein surface over that of  $\text{K}^+$ , indicate why at physiological ionic strengths

the former but not the latter ion can impair the function of proteins in the cell. The energetically expensively maintained concentration differences of sodium and potassium between the interior and exterior of a living cell possibly represent a direct consequence of this fact (11).

## Materials and Methods

### *Computational details*

Structures of all the studied proteins - actin, bovine pancreatic trypsin inhibitor (BPTI), ubiquitin, hyperthermophilic rubredoxin, and ribonuclease (RNase) A were downloaded from the PDB database (27). Oligopeptides (Asp-Ser, Asp-Gly-Ser, (Asp)<sub>10</sub> and (Glu)<sub>10</sub>) were built from scratch using amino acid templates and capped using the acetyl and methylamide groups at the N- and C-termini, respectively. Isolated amino acids (Asp and Glu) were terminated in the same way.

Dissociable groups in the amino acid side chains of the proteins were protonated according to target pH 7 and the resulting structures were solvated in periodic rectangular water boxes, employing the SPC/E water model (28). A sufficiently large cavity was initially carved in the water box in order to accommodate the protein molecule. The net charge of the systems was neutralized by chloride or by sodium and potassium ions. Similar approach was also applied to the oligopeptides under study.

As a next step, equal amounts of NaCl and KCl were introduced into the simulation cell to form an approximately 0.25 M (NaCl) + 0.25 M (KCl) solution. This hyperphysiological concentration was adopted to improve the statistics of the ion-protein contacts. For comparison, proteins in solutions with reduced or increased salt concentrations, as well as those containing only a single salt were also simulated, showing very similar results concerning the Na<sup>+</sup>/K<sup>+</sup> ion specificity at the protein surface. Solvated acetate anion with one Cl<sup>-</sup>, Na<sup>+</sup>, and K<sup>+</sup> ion in the unit cell was created as well. The detailed parameters for individual systems were as follows:

*Actin*. PDB code 1J6Z (monomeric structure). The resulting net charge of -2 e was compensated by 1 Na<sup>+</sup> and 1 K<sup>+</sup> ions. The unit cell of approximate initial dimensions of 91 x 67 x 75 Å contained in addition 12759 water molecules, 58 Na<sup>+</sup>, 58 K<sup>+</sup>, and 116 Cl<sup>-</sup> ions.

*BPTI*. PDB code 6PTI. The resulting net charge of +6 e was compensated by 6 Cl<sup>-</sup> ions. The unit cell of approximate initial dimensions of 41 x 45 x 45 Å contained in addition 2184 water molecules, 10 Na<sup>+</sup>, 10 K<sup>+</sup>, and 20 Cl<sup>-</sup> ions.

*RNase A*. PDB code 1FS3. The resulting net charge of +4 e was compensated by 4 Cl<sup>-</sup> ions. The unit cell of approximate initial dimensions of 51 x 50 x 60 Å contained in addition 4329 water molecules, 19 Na<sup>+</sup>, 19 K<sup>+</sup>, and 38 Cl<sup>-</sup> ions.

*Hyperthermophilic rubredoxin*. PDB code 1BRF. The resulting net charge of -6 e was compensated by 3 Na<sup>+</sup> and 3 K<sup>+</sup> ions. The unit cell of approximate initial dimensions of 43 x 40 x 45 Å contained in addition 2229 water molecules, 10 Na<sup>+</sup>, 10 K<sup>+</sup>, and 20 Cl<sup>-</sup> ions.

*Ubiquitin*. PDB code 1UBQ. The resulting net charge was 0. The unit cell of approximate initial dimensions of 43 x 40 x 45 Å contained in addition 3688 water molecules, 17 Na<sup>+</sup>, 17 K<sup>+</sup>, and 34 Cl<sup>-</sup> ions.

*Ac-(Glu)<sub>10</sub>-NMe*. The resulting net charge of -10 e was compensated by 5 Na<sup>+</sup> and 5 K<sup>+</sup> ions. The unit cell of approximate initial dimensions of 55 x 55 x 55 Å contained in addition 5200 water molecules, 23 Na<sup>+</sup>, 23 K<sup>+</sup>, and 46 Cl<sup>-</sup> ions.

*Ac-(Asp)<sub>10</sub>-NMe*. The resulting net charge of -10 e was compensated by 5 Na<sup>+</sup> and 5 K<sup>+</sup> ions. The unit cell of approximate initial dimensions of 55 x 55 x 55 Å contained in addition 5200 water molecules, 23 Na<sup>+</sup>, 23 K<sup>+</sup>, and 46 Cl<sup>-</sup> ions.

*Ae-Asp-Gly-Ser-NMe*. The resulting net charge was -1 e. The unit cell of approximate initial dimensions of 34 x 34 x 34 Å contained in addition 825 water molecules, 2 Na<sup>+</sup>, 2 K<sup>+</sup>, and 3 Cl<sup>-</sup> ions.

*Ac-Asp-Ser-NMe*. The resulting net charge was -1 e. The unit cell of approximate initial dimensions of 30 x 30 x 30 Å contained in addition 540 water molecules, 2 Na<sup>+</sup>, 2 K<sup>+</sup>, and 3 Cl<sup>-</sup> ions.

*Ac-Glu-NMe*. The resulting net charge was -1 e. The unit cell of approximate initial dimensions of 28 x 28 x 28 Å contained in addition 450 water molecules, 1 Na<sup>+</sup>, 1 K<sup>+</sup>, and 1 Cl<sup>-</sup> ions.

*Ac-Asp-NMe*. The resulting net charge was -1 e. The unit cell of approximate initial dimensions of 28 x 28 x 28 Å contained in addition 450 water molecules, 1 Na<sup>+</sup>, 1 K<sup>+</sup>, and 1 Cl<sup>-</sup> ions.

*Acetate anion*. The resulting net charge was -1 e. The unit cell of approximate initial dimensions of 27 x 27 x 27 Å contained in addition 375 water molecules, 1 Na<sup>+</sup>, 1 K<sup>+</sup>, and 1 Cl<sup>-</sup> ions.

The MD simulations of proteins consisted of minimization, heating to 300 K, 0.5 ns equilibration at constant pressure, and 1 ns production runs in the NpT ensemble. We used the same simulation protocol as in our recent simulations on salt effects on solvated horseradish peroxidase and BPTI (20), which provided converged results for the distribution of ions around proteins. Oligopeptides, isolated amino acids, and the acetate ion were simulated in a similar

way with simulation times extended to 10 ns in the former and 100 ns in the latter two cases. All calculations were carried out using the AMBER8 package (29), employing the parm99 force field (30). An interaction cutoff of 12 Å was applied. Long range electrostatic interactions were accounted for in a standard way using the smooth particle mesh Ewald method (31). The SHAKE algorithm was used for constraining bonds containing hydrogen atoms (32).

The resulting trajectories were analyzed in terms of ion distributions, the integrals of which provided the total number of ions within certain distance from the solute (protein, peptide) surface. The average times the cations spent in the vicinity of the given type of amino acid (within 3.5 Å) residue were also recorded. The individual contact times of the Na<sup>+</sup> and K<sup>+</sup> ions with the protein surface did not exceed 30 % of the total simulation time. Frequent exchanges of surface-bound and bulk ions thus ensured good statistics, which was also confirmed by longer test runs providing the same ion distributions in the vicinity of the protein surface.

Ab initio calculations of ion pairing of Na<sup>+</sup>/K<sup>+</sup> with acetate or formate anions were performed at the MP2/aug-cc-pvtz level. For explicit correlation of all valence and outer core (subvalence) electrons additional core/valence basis functions were added (33). The aqueous solvent was described as a polarizable continuum within the COSMO model (34, 35). All parameters were taken as the default ones except for the ionic radius of sodium, which was reduced by 1.3 % in order to match exactly the experimental difference between hydration free energies of Na<sup>+</sup> and K<sup>+</sup> amounting to 17.5 kcal/mol (36). The free energy of ion pairing was evaluated as the difference between the energy of the solvated contact ion pair and the energies of solvated cation and anion. All geometries were optimized in the gas phase at the same level of theory. For comparison, we also evaluated the energy of the contact ion pair for cation-anion

distance taken as the first maximum on the cation-anion radial distribution function from a classical MD simulation in water. Since the shift in distance was very small, this resulted in negligible (below 0.1 kcal/mol) changes in the relative ( $\text{Na}^+$  vs  $\text{K}^+$ ) free energies of ion pairing. Analogous calculations were also performed for pairing of sodium or potassium with formaldehyde.

### *Experimental details*

Conductivity measurements were performed using a table conductometer Jenway 4330 with a vendor-supplied electrode immersed in 10 ml of solution. Single measurements were performed with 3 digit accuracy. Each of the plotted values (Figure 2) is an average over 3 measurements and the estimated statistical error of the relative changes of conductivity is  $\sim 1\%$ . The small residual conductivity of the pure protein solution (of the order of 100  $\mu\text{S}$ ) was subtracted before evaluating the relative changes.

Samples: Bovine Serum Albumin (BSA) - initial fraction by heat shock, fraction V, Sigma Aldrich, cat. no. A7906. Rnase A - from bovine pancreas, Sigma Aldrich cat. no. R6513. Initial experimental protein concentrations: 10 mg/ml. NaCl and KCl (p. a. grade) were obtained from Lachema. Proteins were dissolved in doubly distilled, deionized water and defined amounts of 1 M stock salt (NaCl or KCl) solutions were added to reach a range of salt concentrations from 0.001 to 0.045 M.

### **Acknowledgements**

Support from the Czech Ministry of Education (grant LC512), from the Granting Agency of the Academy of Sciences (grant IAA400400503 to P. J.) and from the Granting Agency of the

Czech Republic (grant 203/06/1727 to J. V. and 203/05/H001 to L. V.) is gratefully acknowledged. We thank Dr. Pavel Kotrba, Dr. Lucie Marešová, and Prof. František Opekar for technical assistance with the samples and measurements, and Prof. Jan Konvalinka for valuable discussions. We are grateful to the *METACentrum* in Brno for generous allocation of computer time, and the Advanced Biomedical Computing Center, NCI-Frederick for the use of their facilities for part of this work.

## References

- (1) Nightingale, E. R. (1959) *J. Phys. Chem.* **63**, 1381-1387.
- (2) Hofmeister, F. (1888) *Arch. Exp. Pathol. Pharmacol. (Leipzig)* **24**, 247-260.
- (3) Inouye, K. , Kuzuya, K. & Tonomura, B. (1998) *J. Biochem. (Tokyo)* **123**, 847-852.
- (4) Wolff, J., Sackett, D. L. & Knipling, L. (1996) *Protein Sci.* **5**, 2020-2028.
- (5) Vogel, H. J., Drakenberg, T. & Forsen, S. (1983) in *NMR of Newly Accessible Nuclei* (Laszlo, P., ed.) vol. 1, pp. 157-197, Academic Press, New Yoork.
- (6) Darnell, J., Lodish, H. & Baltimore, D. (1990) *Molecular Cell Biology* (Scientific American Books, New York).
- (7) Gumbart, J., Wang, Y., Aksimentiev, A., Tajkhorshid, E. & Schulten, K. (2005) *Curr. Opinion Struct. Biol.* **15**, 423-431.
- (8) Ash, W. L., Zlomislic, M. R., Oloo, E. O. & Tieleman, D. P. (2004) *Biochim. Biophys. Acta – Biomembranes* **1666**, 158-189.
- (9) Chen, H., Wu, Y., Voth, G. A. (2006) *Biophys. J.* **90**, L73-L75.
- (10) Allen, T. W., Andersen, O. S. & Roux, B. (2006) *Biophys. J.* **90**, 3447-3468.
- (11) Collins, K. D. (1997) *Biophys. J.* **72**, 65-76.

- (12) Marcus, Y. (1985) *Ion Solvation* (Wiley, Chichester, UK).
- (13) Omta, A. W., Kropman, M. J., Woutersen, S. & Bakker, H. J. (2003) *Science* **301**, 347-349.
- (14) Collins, K. D. (2004) *Methods* **34**, 300-311.
- (15) Collins, K. D. (2006) *Biophys. Chem.* **119**, 271-281.
- (16) Siu, F. M., Ma, N. L. & Tsang, C. W. (2004) *Chem. Eur. J.* **10**, 1966-1976.
- (17) Arakawa, T. & Timasheff, S. N. (1982) *Biochemistry* **21**, 6545-6552.
- (18) Lin, T. Y. & Timasheff, S. N. (1996) *Protein Sci.* **5**, 372-381.
- (19) Weissenborn, P. K. & Pugh, R. J. (1996) *J. Colloid Interface Sci.* **184**, 550-563.
- (20) Vrbka, L., Jungwirth, P., Bauduin, P., Touraud, D. & Kunz, W. (2006) *J. Phys. Chem. B* **110**, 7036-7043.
- (21) Robertson, T. B. (1911) *J. Biol. Chem.* **9**, 303-326.
- (22) Maldonado, S., Irun, M. P., Campos, L. A., Rubio, J. A., Luquita A., Lostao A., Wang, R. J., Garcia-Moreno, B. & Sancho, J. (2002) *Prot. Sci.* **11**, 1260-1273.
- (23) Dominy, B. N., Perl, D., Schmid, F. X. & Brooks, C. L. (2002) *J. Mol. Biol.* **319**, 541-554.

- (24) Muegge, I., Schweins, T. & Warshel, A. (1998) *Proteins-Struct. Funct. Bioinfo.* **30**, 407-423.
- (25) Curtis, R. A., Ulrich, J., Montaser, A., Prausnitz, J. M. & Blanch, H.W. (2002) *Biotechno. Bioeng.* **79**, 367-380.
- (26) Pinna, M. C., Bauduin, P., Tourand, D., Monduzzi, M., Ninham, B. W. & Kunz, W. (2005) *J. Phys. Chem. B* **109**, 16511-16514.
- (27) Berman, H. M., Westbrook, J., Feng, Z., Gilliland, G., Bhat, T. N., Weissig, H., Shindaylov, I. N. & Bourne, P. E. (2000) *Nucleic Acids Res.* **28**, 235-242.
- (28) Berendsen, H. J. C., Grigera & J. R., Straatsma, T. P. (1987) *J. Phys. Chem.* **91**, 6269-6271.
- (29) Case, D. A., Darden, T. A., Cheatham, III, T. E, Simmerling, C. L., Wang, J., Duke, R. E., Luo, R., Merz, K. M., Wang, B., Pearlman, D. A., Crowley, M., Brozell, S., Tsui, V., Gohlke, H. Mongan, J., Hornak, V., Cui, G., Beroza, P., Schafmeister, C., Caldwell, J. W., Ross, W. S. & Kollman, P. A. (2004) *Amber 8* (University of California, San Francisco).
- (30) Wang, J. M., Cieplak, P. & Kollman, P. A. (2000) *J. Comput. Chem.* **21**, 1049-1074.
- (31) Essmann, U., Perera, L., Berkowitz, M. L., Darden, T., Lee, H. & Pedersen, L. G. (1995) *J. Chem. Phys.* **103**, 8577-8593.

- (32) Ryckaert, J.-P., Ciccotti, G. & Berendsen, H. J. C. (1977) *J. Comput. Phys.* **23**, 327-341.
- (33) Dunning, Jr., T. H. (1989) *J. Chem. Phys.* **90**, 1007-1024.
- (34) Barone, V. & Cossi, M. (1998) *J. Phys. Chem. A* **102**, 1995-2001.
- (35) Cossi, M., Rega, N., Scalmani, G. & Barone, V. (2003) *J. Comp. Chem.* **24**, 669-681.
- (36) Schmid, R., Miah, A. M., Sapunov V. N. (2000) *Phys. Chem. Chem. Phys.* **2**, 97-102.

**Figure captions:**

**Figure 1:** Distribution functions (dotted lines) and cumulative sums, i.e., integrated distribution functions (full lines) of cations in the vicinity of the five investigated proteins, obtained from molecular dynamics simulations. The cumulative sums provide the averaged number of sodium (green) or potassium (blue) ions within a given distance from the protein surface. Results are depicted for the whole protein, as well as detailed for the carboxylate groups, other side chain functional groups, and the protein backbone. Note the larger affinity of  $\text{Na}^+$  over  $\text{K}^+$  to the protein surface and the dominant role of the  $\text{COO}^-$  groups for this effect.

**Figure 2:** Relative changes in measured conductivity upon adding 10 mg/ml of a) RNase A or b) BSA to a solution of NaCl (green) or KCl (blue) of varying concentrations. Note the much stronger conductivity decrease for NaCl compared to KCl for both proteins, which is interpreted in terms of stronger affinity of  $\text{Na}^+$  over  $\text{K}^+$  to the protein surface.

Fig. 1:

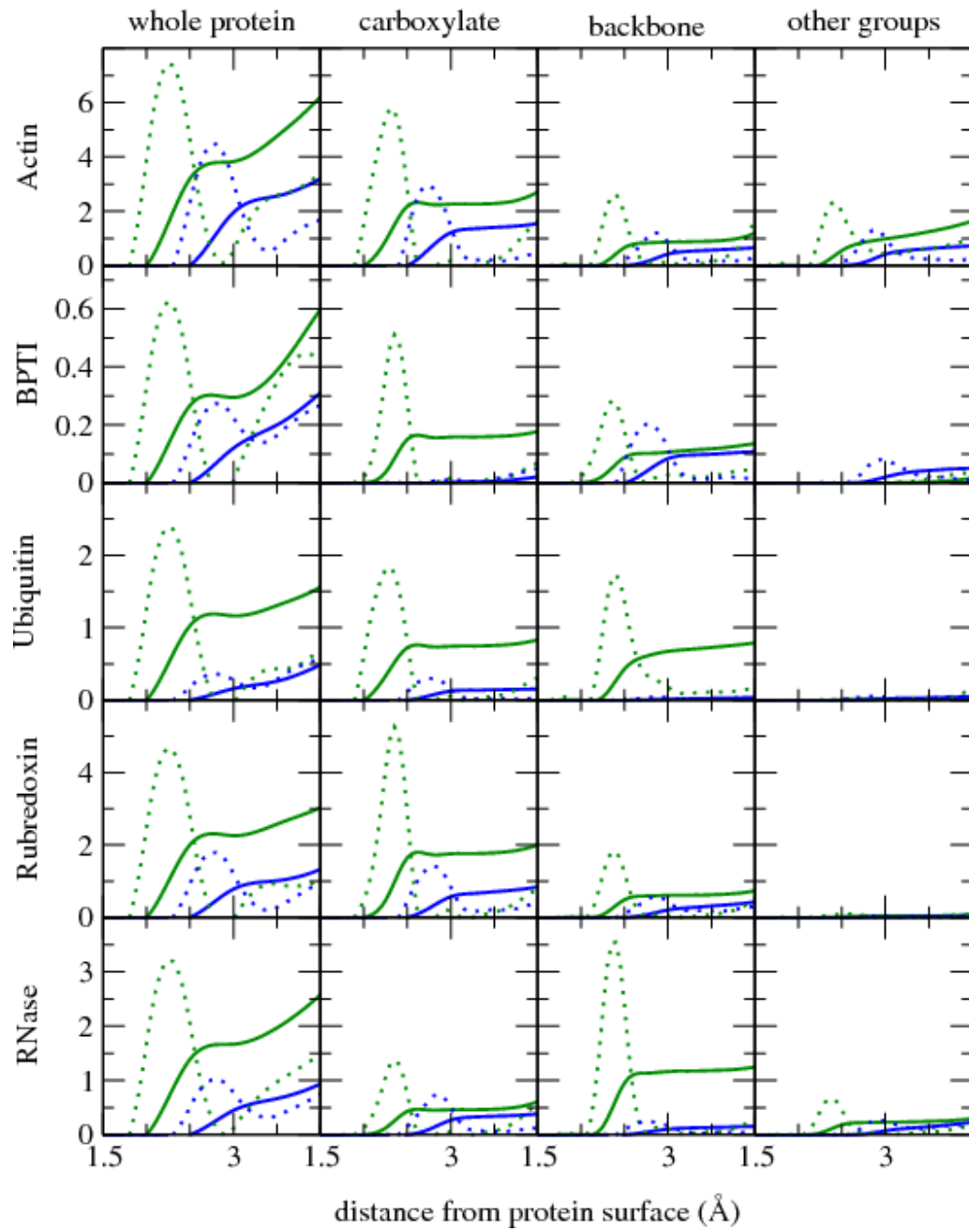
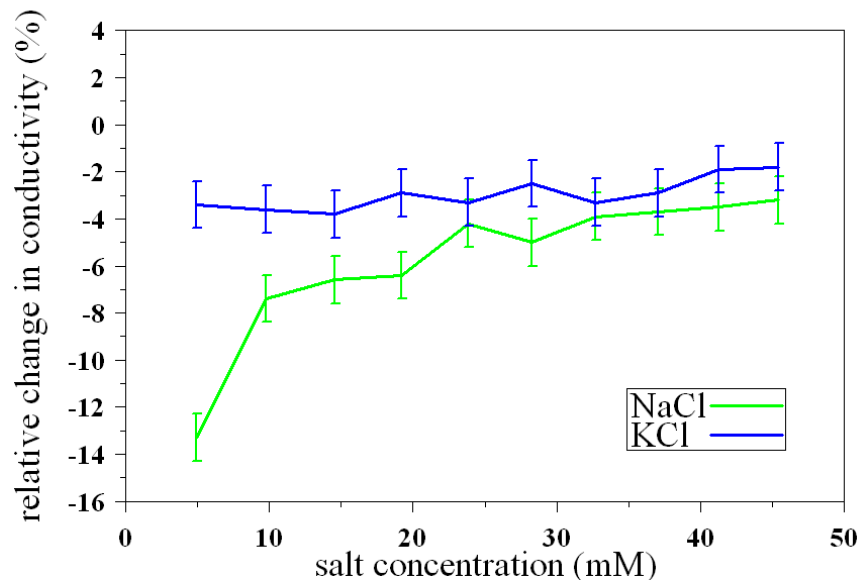
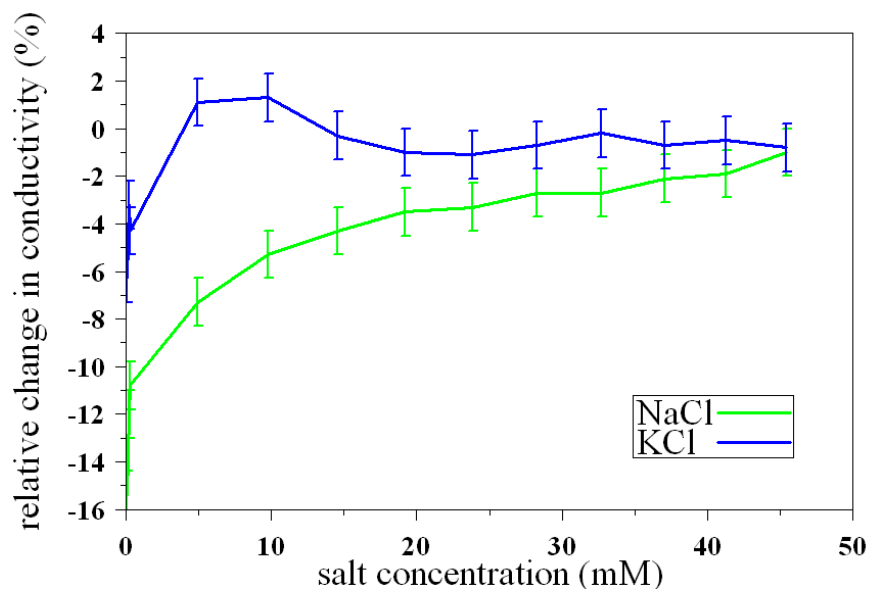


Fig. 2:

(a)



(b)



**Tables:**

**Table 1:**  $\text{Na}^+/\text{K}^+$  ratio in the vicinity of solvated oligopeptides, single aspartate or glutamate, and acetate anion. The oligopeptides and single aminoacids are terminated by acetyl (Ac) and methylamide (NMe) groups.

<b>system</b>	<b><math>\text{Na}^+/\text{K}^+</math> ratio (side chain)</b>	<b><math>\text{Na}^+/\text{K}^+</math> ratio (backbone)</b>
Ac-(Glu) <sub>10</sub> -NMe	2.3	4.0
Ac-(Asp) <sub>10</sub> -NMe	3.5	4.5
Ac-Asp-Gly-Ser-NMe	2.9	2.5
Ac-Asp-Ser-NMe	2.4	2.0
Ac-Glu-NMe	4.8	1.1
Ac-Asp-NMe	2.3	1.8
Acetate anion	3.4	-

**Table 2:** Difference between association free energies of aqueous sodium-carboxylate and potassium-carboxylate ion pairs, where carboxylate is a formate or acetate anion. The results clearly show the preference of Na<sup>+</sup> over K<sup>+</sup> to pair in water with carboxylate anions.

system	$\Delta\Delta G_{K^+ \text{-carboxylate}^- \rightarrow Na^+ \text{-carboxylate}^-}$ (kcal/mol)
formate	-2.58
acetate	-2.22